Results in Physics 7 (2017) 4264–4268

Contents lists available at ScienceDirect

Results in Physics

journal homepage: www.journals.elsevier.com/results-in-physics

Performance of conversion efficiency of a crystalline silicon solar cell with base doping density

Gokhan Sahin [a,*], Genber Kerimli [a], Fabe Idrissa Barro [b], Moustapha Sane [b], Mehmet Hakkı Alma [c]

[a] Electric and Electronic Engineering Department, IĞDIR University, Iğdır 76000, Turkey
[b] Semiconductors and Solar Energy Laboratory, Faculty of Science and Technique, Cheikh Anta Diop Universtity, BP5005 Dakar, Senegal
[c] Industrial Engineering Forestry Department, Kahramanmaras Sutcu Imam University, K. Maras 46060, Turkey

ARTICLE INFO

Article history:
Received 27 July 2017
Received in revised form 17 October 2017
Accepted 18 October 2017
Available online 21 October 2017

Keywords:
Crystalline silicon solar cell
Base doping density
Series resistance
Shunt resistance
Conversion efficiency

ABSTRACT

In this study, we investigate theoretically the electrical parameters of a crystalline silicon solar cell in steady state. Based on a one-dimensional modeling of the cell, the short circuit current density, the open circuit voltage, the shunt and series resistances and the conversion efficiency are calculated, taking into account the base doping density. Either the I-V characteristic, series resistance, shunt resistance and conversion efficiency are determined and studied versus base doping density. The effects applied of base doping density on these parameters have been studied. The aim of this work is to show how short circuit current density, open circuit voltage and parasitic resistances are related to the base doping density and to exhibit the role played by those parasitic resistances on the conversion efficiency of the crystalline silicon solar.

Introduction

Solar cells are semiconductor devices that are able of direct conversion of light into DC electric power. Space research and the need of clean and renewable energies have led to a rapid growth of the production and use of solar cells. In that way, a solar cell technologies has been developed like thin films, organic solar cells, crystalline silicon solar cells, nanowire solar cells, quantum dot solar cells and so on. Since their introduction [1] these devices have been improved to minimize electrical and optical losses leading to a significant increase in their performance [2–4]. This increase of the solar cell performance is directly related to a better knowledge of some important parameters and the technological processes when designing these optoelectronic devices. Many characterization methods in steady state as well as in transient state or frequency modulation were developed for the determination of one or several parameters of the solar cell.

In this work, the electrical parameters of a silicon solar cell are investigated theoretically using a one dimensional model [3,5]. The purpose of the work is to show how solar cell electrical parameters are related to the base doping density and to exhibit the role played by the parasitic resistances on the conversion efficiency of the solar cell. To make this possible, the short circuit current density, the open circuit voltage the shunt and series resistances and the conversion efficiency are calculated taking into account the base doping density.

Mathematical development

A schematic diagram of the $n^{+-}p\text{-}p^{+}$ crystalline silicon solar cell showing the different coordinates is given in Fig. 1. H is the base thickness and x the depth in the base of the solar cell.

This study is conducted under some assumptions:

- The emitter contribution is neglected given that the base has a greater contribution to photocurrent.
- The base is quasi-neutral, we are in low injection condition with no lateral effect; the principal transport mechanism is then a one-dimension diffusion of minority carriers.

Excess minority carrier density: Carrier generation, recombination and drift/diffusion are the three major phenomena that occur inside the solar cell under illumination; in steady state the transport equation can be written as:

$$\frac{\partial^2 \delta(x)}{\partial x^2} - \frac{\delta(x)}{L^2} = -\frac{G(x)}{D} \tag{1}$$

with $\delta(x)$ the excess minority carrier density, L their diffusion length and D their diffusion coefficient and $G(x)$ the carrier generation rate

* Corresponding author.
E-mail address: gokhan.sahin@igdir.edu.tr (G. Sahin).

https://doi.org/10.1016/j.rinp.2017.10.039
2211-3797/

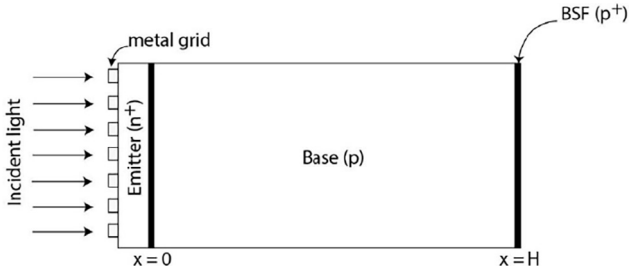

Fig. 1. n^+pp^+ crystalline silicon solar cell.

at the depth x in the base. The diffusion coefficient is related to the base doping density Nb trough Eq. (2) [6].

$$D_0(N_b) = \frac{1350.V_t}{\sqrt{1+\frac{81.N_b}{(N_b+3{,}2.10^{18})}}} \tag{2}$$

Minority carriers lifetime is also directly related to the base doping density Nb by [6].

$$\tau_0(N_b) = \frac{12}{1+\frac{N_b}{5.10^{16}}}(\mu s) \tag{3}$$

The minority carrier diffusion length L of the excess minority carriers depends on base doping rate by the following expression:

$$L(N_b) = \sqrt{D(N_b).\tau(N_b)} \tag{4}$$

Under back side illuminated, the expression of generation rate is given by the relation (5): The silicon solar cell is used in static regime [7,8].

$$G(x) = n \cdot \sum_{m=1}^{3} a_m . \exp(-b_m . x) \tag{5}$$

Coefficients a_m and b_m are tabulated values obtained from AM1.5 solar radiation and the dependence of the absorption coefficient on the illumination wavelength, n = 1 (Number of sun). [7,9]. Solution of equation Eq. (1) can be written as:

$$\delta(x) = C1.\exp\left(\frac{x}{L}\right) + C2.\exp\left(-\frac{x}{L}\right) + \sum_{m=1}^{3} K_m.\exp(-b_m.x) \tag{6}$$

The coefficient C1 and C2 the final solution of the continuity equation. The coefficients C1 and C2 can be determined by considering the two following boundary conditions:

- at the junction (x = 0):

$$\left.\frac{\partial\delta(x)}{\partial x}\right|_{x=0} = \frac{Sf}{D}.\delta(0) \tag{7}$$

- at the back junction (x = H):

$$\left.\frac{\partial\delta(x)}{\partial x}\right|_{x=H} = -\frac{Sb}{D}.\delta(H) \tag{8}$$

where H is the total thickness of the solar cell, Sb and Sf are respectively the back surface recombination velocity and the junction dynamic velocity [10,11].

Short circuit current density: From the minority carrier density, we can derive the photocurrent density as:

$$Jph = q.D.\left.\frac{\partial\delta(x)}{\partial x}\right|_{x=0} \tag{9}$$

The short circuit current density is then obtained for high values of the junction dynamic velocity Sf:

$$Jsc = J_{ph}\big|_{Sf\to\infty} \tag{10}$$

q is the electronic charge.

Open circuit voltage: The Photovoltage across the junction comes from the Bolzmann relation:

$$V_{ph} = V_T.\ln\left(\frac{N_b.\delta(x=0)}{n_i^2}+1\right) \tag{11}$$

With V_T the thermal voltage, Nb the base doping density and ni the intrinsic concentration.

The open circuit voltage is obtained for very low dynamic junction velocity Sf:

$$V_{oc} = V_{ph}\big|_{Sf\to 0} \tag{12}$$

Based on both the photocurrent density and the photovoltage, the output power per unit area is written as:

$$P_{ph} = V_{ph}J_{ph} \tag{13}$$

The diode current has been neglected in the above equation. From that expression of the power output, we can derive the maximum power output of the cell Pmax allowing us to calculate the conversion efficiency.

Conversion efficiency: The conversion efficiency of the solar cell is defined by:

$$\eta = \frac{P_{\max}}{P_{inc}} \tag{14}$$

with P_{inc} the corresponding incident power. The dependence of the conversion efficiency on base doping density can also get affected if the values of the cell parameters like shunt resistance (Rsh) and series resistance (Rs) themselves change with base doping. To know more about those dependencies, we have to determine both series and shunt resistances. To do that, let us consider the two following figures, Figs. 2-a and 2-b and Figs. 3-a and 3-b where the solar cell is illuminated [12,13].

The shunt resistance comes from the recombination of charge carriers in volume, surface (hanging links and manufacturing technology) and possible short circuits at the junction of the photovoltaic cell. It is also indicative of a good quality of a solar cell because when it is large or small, the leakage current through the solar cell is low or large. Let us now consider the current-voltage characteristic of the photovoltaic cell (Fig. 2a), in particular in the vicinity of the short-circuit operation.

For determine the shunt resistance Rsh, the equivalent electrical model of the solar cell in short circuit (high Sf values (4.10^4

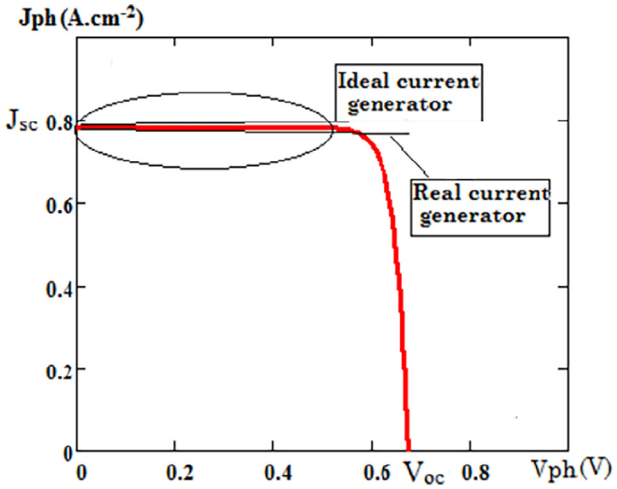

Fig. 2(a). Illuminated I-V curve for the shunt resistance.

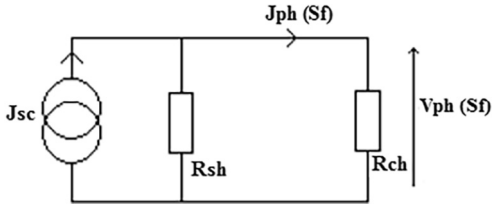

Fig. 2(b). Corresponding equivalent electrical circuit near short circuit.

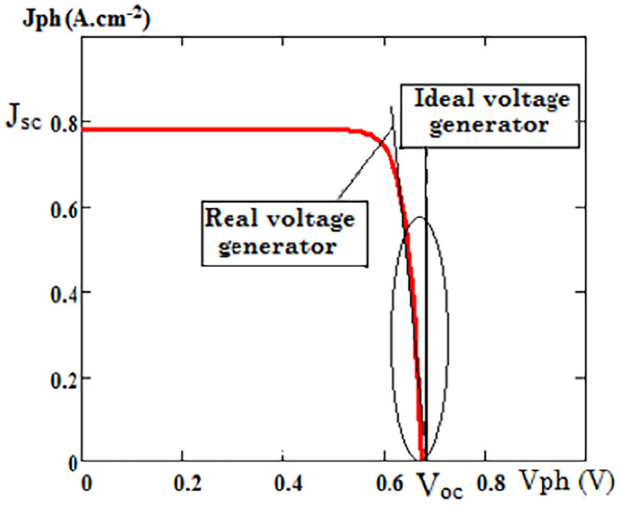

Fig. 3(a). Illuminated I-V curve for the series resistance.

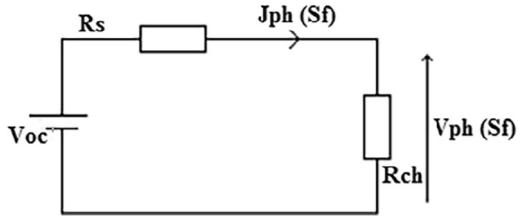

Fig. 3(b). Corresponding equivalent electrical circuit near open circuit.

$cm{\cdot}s^{-1} < Sf < 6.10^6\ cm{\cdot}s^{-1}$) is proposed. In short circuit situation the solar cell is presented as current generator in parallel with the shunt resistance and with the external charge resistance R_{ch} [14]. The illustrative model of this device is given to the Fig. 2(b):

Where, Jsc is the short-circuit photocurrent; the 10th expression is determined, Rsh: shunt resistance per unit area, Jph et Vph: density current et photovoltage, Rch: Charge resistance. The series resistance, one of the fundamental electrical parameters depending on the nature of the substrate, the temperature and the technology used, plays a decisive role in the quality of a photovoltaic cell. It characterizes the resistive effects of the quasi-neutral regions of the photovoltaic cell, metal contacts and metal/semiconductor contacts Consider the current-voltage characteristic of the photovoltaic array (Fig. 3a), particularly in the vicinity of open-circuit operation.

For determining the series resistance Rs, we propose the equivalent electrical model of the solar cell in open circuit (low values of Sf) where the solar cell operates as photovoltage generator associated to series resistance and the external charge resistance (R_{ch}) [15].

The equivalent electrical model of the solar cell near open circuit is represented below:

Voc: open circuit voltage, Rs: Series resistance per unit area, Vph: voltage. The series resistance Rs is caused by the movement of electrons through the emitter and base of the cell, the contact resistance between the metal contact and the silicon and the resistance of metal grids at the front and the rear of solar cell. Fig. 2a shows that when the solar cell operates near short circuit, which is for higher values of Sf, it behaves like a real current generator and then can be represented as an ideal current generator Jsc shunted by a parasitic resistance Rsh as presented in Fig. 2b. Based on Fig. 2b, we can write that:

$$Vph(Sf) = \mathrm{Rsh}.[J_{sc} - J_{ph}(Sf)] \tag{15}$$

This equation can be rearranged leading to an expression of the shunt resistance Rsh in the form [12]:

$$Rsh(Sf) = \frac{V_{ph}(Sf)}{J_{sc} - J_{ph}(Sf)} \tag{16}$$

Since this expression has been determined near short circuit, it holds only for high Sf [15] values.

On Fig. 3a, considering now that the solar cell operates near open circuit, we can see on this I-V curve that it behaves like a real generator; thus this corresponds to an ideal voltage generator in series with a parasitic resistance (Rs) as presented on Fig. 3b. From Kirchhoff law applied to Fig. 3b, we have:

$$Rs.Jph(Sf) = V_{oc} - V_{ph}(Sf) \tag{17}$$

We then deduce that:

$$Rs(Sf) = \frac{V_{oc} - V_{ph}(Sf)}{J_{ph}(Sf)} \tag{18}$$

Contrary to Eq. (16) this above equation holds only for very low Sf values.

Results and discussion

From the mathematical formulation presented above, simulations were performed for various base doping densities.

Shunt and series resistances: The two resistors model internal losses [16] :- Series Resistance Rs: models the ohmic losses in the material. Shunts Resistance Rsh: models the parasitic currents traversing the cell. We present here some simulation results obtained from the previously described model. We evaluated the parasitic resistances, that is shunt and series resistances and the resulted curves are presented on Fig. 4.

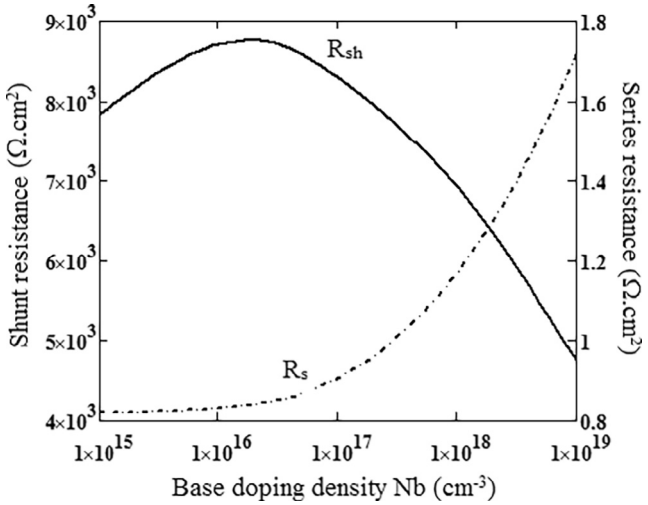

Fig. 4. Shunt and series resistances versus base doping.

Fig. 4 shows clearly that series resistance is an increasing function of base doping density. This phenomenon increases the ability of materials to resist the passage of electric current. Thus there for a base doping density gradient is an increase in resistivity of semiconductor material, the constituent metal contacts the electrodes and the grid of the minority carrier collection. Since the amount of free carriers decrease with base doping, the apparent mobility of that carriers decrease leading to the observed increase of series resistance for shunt resistance, there is firstly and increase followed by a marked decrease. The insertion of impurities first diminishes the amount of free carriers so that shunt resistance firstly increase; after a certain threshold, there are also more and more defects that induce current losses in the base: the solar cell then behaves as short circuited. Thus the leakage current is reduced: it is said that the shunt resistance is high.

Open circuit voltage and short circuit current density: We present on Fig. 5 the open circuit voltage and the short circuit current density versus base doping.

This figure (Fig. 5) shows that open circuit voltage increase with base doping contrary to the short circuit current density. Effectively, for increasing base doping, there are more and more impurities in the base, that is more and more defect also; Generated carriers are trapped by these defects leading to less and less free carriers that can cross the junction: the collected current then decrease. In the same time the amount of fixed charge in the neighborhood of the junction increase. That is why the open circuit voltage increase with base doping. These curves also suggest that an optimal base doping should exist (in the range of 10^{17} cm^{-3}) where both open circuit voltage and short circuit current density are sufficiently high.

Conversion efficiency: In Figs. 6(a) and 6(b), we plotted the conversion efficiency versus series resistance (a) and next versus shunt resistance [17].

The conversion efficiency of the bifacial cell has also been evaluated for front, rear and bifacial illumination. The obtained curves are presented on Fig. 6(a). This figure shows that the conversion efficiency of the solar cell decreases with base doping density as recombination processes increase with base doping density. The bifacial efficiency is more important compared to that of the commonly front illumination, as expected. This is due to the contribution of the rear illumination; note that rear illumination condition should be improved (passivation of the rear side, back surface field BSF, ground surface reflection properties) to gain effect of bifacial illumination. We supposed here that for rear illumination we have the same incident flux. Really this may be wrong due to different factors [18–20]. To evaluate more accurately the bifacial efficiency,

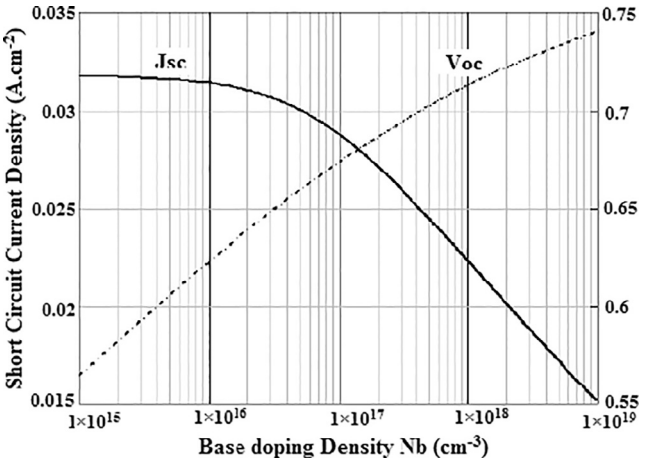

Fig. 5. Open circuit voltage and short circuit current density versus base doping.

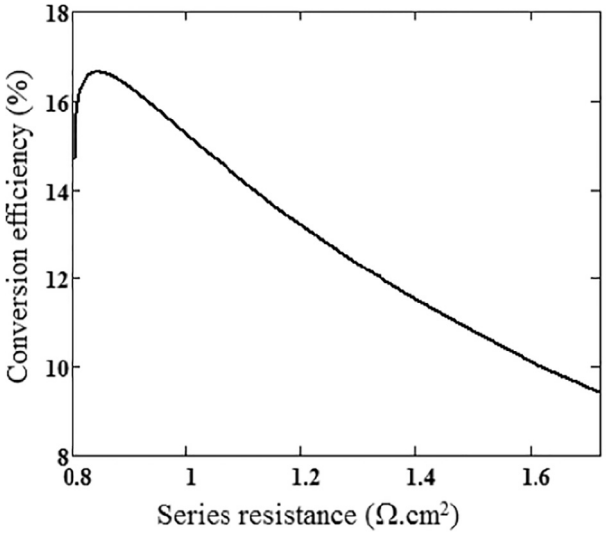

Fig. 6(a). Conversion efficiency versus series resistance.

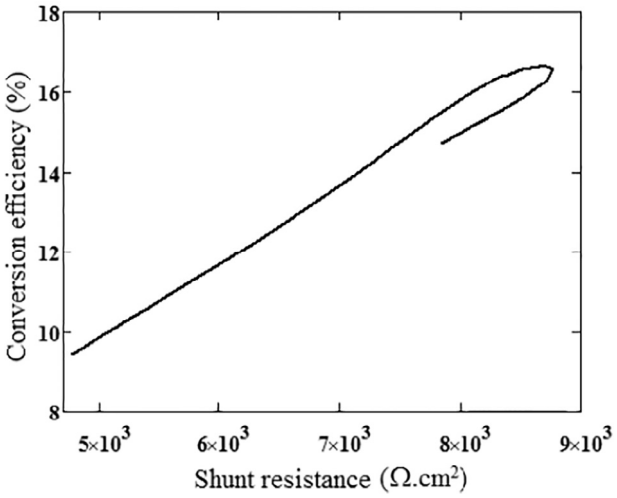

Fig. 6(b). Conversion efficiency versus shunt resistance.

we then varied the rear incident flux (rear factor). The resulting dependencies are plotted on Fig. 6(b).

We can observe on Fig. 6a that the conversion efficiency first increase before decreasing with base doping. This also suggest an optimal value of the series resistance. For increasing series resistance, the voltage at the output will be severely limited so that the output power will decrease for an unchanged incident power. That is, the conversion efficiency will decrease, as observed on the figure.

On Fig. 6b we have an increase of the conversion efficiency with the shunt resistance. Effectively, increasing Rsh means that there are less and less carrier loss in the solar cell and then an increase of the output current. There is then an increase of the output power, that is, of the conversion efficiency.

Conclusion

A theoretical investigation of the electrical parameters of a crystalline silicon solar cell in steady state has been made. We showed that short circuit current density as well as the shunt resistance and conversion efficiency decrease with base doping density con-

trary to open circuit voltage and series resistance. The conversion efficiency decreases with series resistance and increases with shunt resistance. The I-V characteristic was represented, this allowed us to establish the expressions of series and shunt resistances following both modes of functioning of the solar cell (open circuit situation and short-circuit situation). These modes were also studied according to the junction recombination velocity for various base doping density. These results showed explicitly the exact behavior of the solar cell for the studied parameters. We demonstrated that base doping density plays an important role on the performance of the crystalline silicon solar cell.

Appendix A. Supplementary data

Supplementary data associated with this article can be found, in the online version, at https://doi.org/10.1016/j.rinp.2017.10.039.

References

[1] Mori H, 1966. Radiation energy transducing device. U. S.
[2] Untila GG, Kost TN, Chebotareva AB, Zaks MB, Sitnikov AM, Solodukha OI, et al. Bifacial low concentrator argentum free crystalline silicon solar cells based on ARC of TCO and current collecting grid of copper wire. AIP Conf Proc 2013;1556:106.
[3] Topkaya R. Effect of composition and temperature on the magnetic properties of BaBixLaxFe(12-2x)O19 (0.0 = x = 0.2) hexaferrites. Appl Phys A 2017. https://doi.org/10.1007/s00339-017-1115-y.
[4] Moehlecke A, Osório VC, Zanesco I. Analysis of thin bifacial silicon solar cells with locally diffused and selective back surface field. Mater Res 2014.
[5] Topkaya R. Ferromagnetic resonance study of Fe/Cu multilayer thin film. J Supercond Nov Magn 2017;30:1275–80. https://doi.org/10.1007/s10948-016-3920-5.
[6] Liou JJ, Wong WW. Comparison and optimization of the performance of Si and GaAs solar cells. Sol Energy Mater Sol Cells 1992;1(28):9–28.
[7] Furlan J, Amon S. Approximation of the carrier generation rate in illuminated silicon. Solid-State Electron 1985;12(28):241–1243.
[8] Mohammad SN. An alternative method for the performance analysis of silicon solar cells. J Appl Phys 1987;61(2):767–72.
[9] Rajman K, Singh R, Shewchun. Absorption coefficient of silicon for solar cell calculations. J Solid-State Electron 1979;22:793–5.
[10] Sahin G. Effect of temperature on the series and shunt resistance of a silicon solar cell under frequency modulation. J Basic Appl Phys 2016;5(1):21–9.
[11] Ndiaye EH, Sahin G, Moustapha D, Amary T, Hawa LD, Mor N, et al. Study of the intrinsic recombination velocity at the junction of silicon solar under frequency modulation and irradiation. J Appl Math Phys 2015;3:1522–35.
[12] Sahin G. Effect of incidence angle on the electrical parameters of vertical parallel junction silicon solar cell under frequency domain. Moscow Univ Phys Bull 2016;71(5):498–507.
[13] Şahin G, Barro FI, Sané M, Honadia PAH, Kocyigit A, Kerimli G. Performance of conversion efficiency of a bifacial silicon solar cell with particle irradiation. Chin J Phys 2016:1–8.
[14] Sow E, Mbodjil S, Zouma B, Zoungrana M, Zerbo I, Sere A, Sissoko G. Determination in 3D modeling study of the width emitter extension region of the solar cell operating in open circuit condition by the Gauss's Law, Int J Sci Environ Technol (IJSET), 1; N4.
[15] Kotsovos K, Misiakos K, 16th European Photovoltaic Solar Energy Conference, 1–5 May 2000, Glasgow, UK.
[16] Samer S, Ahmed M, Mohieddine B, Shehab AA. Matlab/simulink-based photovoltaic array model employing simpowersystems toolbox. J Energy Power Eng 2012;6:1965–75.
[17] Sahin G. Effect of wavelength on the electrical parameters of a vertical parallel junction silicon solar cell illuminated by its rear side in frequency domain. Results Phys 2016;6(2016):107–11.
[18] Sugibuchi K, Ishikawa N, Obara S. Bifacial-PV Power Output Gain in the Field Test Using "Earthon" High Bifaciality Solar Cells. Proceedings of the 28th European Photovoltaic Solar Energy Conference, Paris (France). 2013; pp. 4312–4317.
[19] Grigorieva G, Kagan M, Unishkov V, Zviagina K, Kreinin L, Bordin N, Broder J, Eisenberg Y, Eisenberg N. Efficiency of bifacial si solar cells at low irradiance. effect of design and fabrication technology factors. In: Proceedings of the 25th European Photovoltaic Solar Energy Conference/5th World Conference on Photovoltaic Energy Conversion, Valencia (Spain). 2010; pp. 1805–1809.
[20] Sahin G, Moustapha D, Mohamed AOEM, Moussa IN, Amary T, Grégoire S. Capacitance of vertical parallel junction silicon solar cell under monochromatic modulated illumination. J Appl Math Phys 2015;3:1536–43.